Published in final edited form as:
J Immunol. 2012 April 1; 188(7): 3496–3505. doi:10.4049/jimmunol.1103182.

ERK2-Dependent Activation of c-Jun is Required for Nontypeable *H. influenzae*-Induced CXCL2 Up-Regulation in Inner Ear Fibrocytes

Sejo Oh[*,1], **Jeong-Im Woo**[*,1], **David J. Lim**[*,†], and **Sung K. Moon**[*]

[*]Division of Clinical and Translational Research, House Research Institute, Los Angeles, CA 90057

[†]Department of Cell and Neurobiology, Keck School of Medicine, University of Southern California, Los Angeles, CA 90089

Abstract

The inner ear, composed of the cochlea and the vestibule, is a specialized sensory organ for hearing and balance. Although the inner ear has been known as an immune-privileged organ, there is emerging evidence indicating an active immune reaction of the inner ear. Inner ear inflammation can be induced by the entry of pro-inflammatory molecules derived from middle ear infection. Since middle ear infection is highly prevalent in children, middle ear infection-induced inner ear inflammation can impact the normal development of language and motor coordination. Previously, we have demonstrated that the inner ear fibrocytes (spiral ligament fibrocytes) are able to recognize nontypeable *Haemophilus influenzae* (NTHi), a major pathogen of middle ear infection, and up-regulate a monocyte-attracting chemokine through TLR2-dependent NF-κB activation. Here, we aimed to determine molecular mechanism involved in NTHi-induced cochlear infiltration of polymorphonuclear cells. The rat spiral ligament fibrocytes (SLFs) were found to release CXCL2 in response to NTHi via activation of c-Jun, leading to the recruitment of polymorphonuclear cells to the cochlea. We also demonstrated that MEK1/ERK2 signaling pathway is required for NTHi-induced CXCL2 up-regulation in the rat SLFs. Two AP-1 motifs in the 5'-flanking region of CXCL2 appeared to function as a NTHi-responsive element, and the proximal AP-1 motif was found to have a higher binding affinity to NTHi-activated c-Jun than the distal one. Our results will enable us to better understand the molecular pathogenesis of middle ear infection-induced inner ear inflammation.

Introduction

The inner ear, a sensory organ for hearing and balance, is composed of various types of cells such as sensory hair cells and non-sensory supporting cells (1, 2). Like the brain and the eyes, the inner ear has been known as an immune-privileged organ associated with a blood-labyrinthine barrier (3, 4). However, there is emerging evidence that the inner ear is not an immunologically inactive organ. Tissue resident macrophages were found to constitutively exist in the spiral ligament and spiral ganglion of the cochlea (5). The external sulcus cells of the cochlea also appeared to express a pathogen recognition receptor, Toll-like receptor 4 (TLR4) (6). Moreover, the fibrocytes in the spiral ligament (SLFs) are known to respond to a systemic challenge of endotoxin (7).

Corresponding author: Sung K. Moon Address: 2100 West 3rd Street, Los Angeles, CA 90057 Tel: (213) 273-8081 Fax: (213) 273-8088 smoon@hei.org.

[1]S. O. and J. -I. W. contributed equally to this work.

The SLFs, the most abundant inner ear cell type, express a variety of ion channels such as Na^+/K^+-ATPase and connexin 26 (8, 9) serving as a part of the potassium recycle pathway required for normal hearing (10, 11). According to the ion channels expressed, the SLFs are divided into several types (12). Interestingly, one type of the SLFs activates NF-κB in response to noise exposure, whereas another type mainly responds to a systemic challenge of lipopolysaccharide (LPS) (7). The SLFs can release inflammatory mediators in response to pro-inflammatory cytokines (13) and otitis media (OM) pathogens such as *S. pneumoniae* and nontypeable *H. influenzae* (NTHi) (14).

OM is one of the most common pediatric infectious diseases, which is attributed to physician visits more than 20 million per annum in the USA (15). As a complication, OM can lead to inner ear inflammation, i.e. serous and purulent labyrinthitis (16), resulting in sensorineural hearing loss (SNHL) (17) and vertigo (18). OM-induced inner ear inflammation in children are clinically important since they can result in a delay in the development of language (19) and motor coordination (20). However, it is not easy to detect OM-induced SNHL with a conventional hearing test because it is frequently transient and limited in the ultra-high frequency (21, 22).

OM-induced inner ear inflammation is evoked by the entry of bacterial molecules of OM pathogens into the inner ear through the round window membrane (23). It has been demonstrated that pneumococcal OM results in hair cell loss (24) and pathologic changes in the cochlear lateral wall (25, 26) in the animal studies. However, molecular mechanism involved in OM-induced inner ear inflammation remains unclear. Recently, we have shown that the SLFs induce MCP-1/CCL2 in response to NTHi through TLR2-dependent NF-κB activation (27), and SLF-derived MCP-1/CCL2 is involved in CCR2-mediated cochlear infiltration of monocytes (28). However, we poorly understand how the SLFs contribute to the recruitment of polymorphonuclear leukocytes (PMNs).

Among PMN-attracting chemokines, we showed that CXCL2, also known as macrophage inflammatory protein-2, is highly up-regulated in the SLFs in response to OM pathogens (14). CXCL2, which is associated with inflammatory diseases such as arthritis, glomerulonephritis, and sepsis (29-31), is up-regulated by LPS through the activation of both NF-κB and c-Jun in the murine macrophages (32). Pyrrolidine dithiocarbamate induces CXCL2 only via c-Jun-dependent signaling pathway (33), whereas Sp-1 is involved in CXCL2 up-regulation in response to both CpG-oligodeoxynucleotide and LPS (34). Since these results suggest that a signaling pathway required for CXCL2 induction varies according to the pro-inflammatory signals, we aimed to determine a signaling pathway involved in NTHi-induced CXCL2 up-regulation in the SLFs.

We here show that the MEK1-dependent phosphorylation of ERK2 is involved in NTHi-induced CXCL2 up-regulation in the SLFs. We demonstrated that the SLFs require c-Jun for the up-regulation of CXCL2 in response to NTHi, and two AP-1 motifs of CXCL2 function as a NTHi-responsive element. In addition, we found that the proximal AP-1 motif has a higher binding affinity to NTHi-activated c-Jun compared to the distal one. We expect that our findings will enable us to further understand the molecular pathogenesis of OM-induced inner ear inflammation and provide us with a novel strategy for the prevention of inner ear complication secondary to middle ear inflammation.

Materials and Methods

Reagents

PD98059, SP600125, AG126, and FR180204 were purchased from Calbiochem (San Diego, CA). SB203580 was purchased from Tocris (Ellisville, MO). Tanshinone IIA, nicotinamide

adenine dinucleotide (NAD) and hemin were purchased from Sigma-Aldrich (St. Louis, MO). TaqMan primers and probes for rat *CXCL2* (Rn00586403) and rat *GAPDH* (glyceraldehyde-3-phosphate dehydrogenase) (4352338E) were purchased from Applied Biosystems (Foster City, CA).

Bacterial culture and preparation of bacterial lysate

NTHi strain 12, originally a clinical isolate from the middle ear fluid of a child with acute OM, was used in this study (35). The NTHi lysate was prepared as described previously (36). Briefly, a single colony of NTHi was harvested from a chocolate agar plate, inoculated into 3 ml of brain heart infusion (BHI) broth supplemented with NAD and hemin (both at 10 μg/ml) and placed in a shaking incubator overnight. After addition of 50 ml of fresh BHI broth, bacteria were further grown for 4 h to a mid-log phase (A_{600} = 0.5 to 0.7). The supernatant was discarded after centrifugation at 10,000 × *g* for 10 min. The bacterial pellet was resuspended in 10 ml of phosphate-buffered solution (PBS) and sonicated to lyse bacteria. The lysate was then centrifuged at 10,000 × *g* for 10 min and the supernatant was collected. The protein concentration of the NTHi lysate was determined using the BCA™ protein assay kit (Pierce Biotechnologies, Rockford, IL).

Animal Experiments

C57BL/6 and *Cxcr2*$^{-/-}$ mice (B6.129S2(C)-*Cxcr2*^{tm1Mwm}) were purchased from the Jackson Laboratory (Bar Harbor, MA). All animal experiments were approved by the Institutional Animal Care and Use Committee of the House Research Institute. 10^7 cfu of live NTHi was suspended in 10 μl of saline and was transtympanically inoculated into the middle ear of the young adult male mice using a 30 G needle and syringe under the surgical microscope. As a control, normal saline was inoculated with the same procedure. Animals were sacrificed 5 days after inoculation, and temporal bones were dissected. After fixation and decalcification, the temporal bones were embedded in paraffin and were serially sectioned through the mid-modiolar plane at a thickness of 5 μm. H & E staining was performed on the every 10th to 20th section for the histological analysis.

For immunolabeling, endogenous peroxidase activity was quenched with incubation in 0.3% H_2O_2 for 30 min after tissue sections were deparaffinized and rehydrated through an identical series of graded xylene and alcohol solutions. Nonspecific binding sites were blocked by preincubation with a 1:10 dilution of a horse serum for 1 h at room temperature. The polyclonal rabbit anti-CXCL2 antibody (1:200; Santa Cruz Biotechnology Inc. Santa Cruz, CA) was incubated with the sample for 1 h at room temperature. The sections were washed with PBS three times and incubated with a 1:500 dilution of the biotinylated anti-rabbit immunoglobulin G (IgG) antibody (Vector Laboratories, Burlingame, CA) for 30 min at room temperature. Peroxidase was attached by the avidinbiotin complex method, and signals were detected with diaminobenzidine tetrahydrochloride.

Cell culture

The rat SLF cell line (RSL) (37) and murine primary SLFs were used in this study. The RSL cells were maintained in Dulbecco's modified Eagle's medium (DMEM) (Invitrogen, Carlsbad, CA) supplemented with 10% fetal bovine serum, penicillin (100 units/ml), and streptomycin (0.1 mg/ml). Primary SLFs were cultured from explants of the mouse cochlear lateral walls as described (27). Briefly, mouse pups (P3~P6) were euthanatized in a CO_2 chamber and then decapitated. The cochlea was isolated with preservation of its normal structure after dissecting the inner ear from the skull base. After removal of the bony otic capsule, the spiral ligaments were separated from the surrounding tissue (stria vascularis, organ of Corti, and Reissner's membrane) using fine forceps. Explants of the spiral ligaments were plated onto the plastic culture dishes in DMEM supplemented with 10%

fetal bovine serum. After proliferation of the primary cells, the explants were removed. All subcultured cells were spindle-shaped and anchorage-dependent with expression of Ca^{2+} ATPase like a type 1 SLF (38). Primary cells of passage 5 or less were used in this study. All cells were maintained at 37°C in a humidified atmosphere of 5% CO_2 and 95% air.

Migration assays

After 4 ~6 h starvation, the RSL cells were exposed to the NTHi lysate (0.1 μg/ml) for 24 h and the conditioned medium was collected. As a control, the conditioned medium of the RSL cells was separately collected without NTHi exposure. Migration assays were performed using a 24-well plate with polycarbonate membrane inserts (Millipore, Billerica, MA) as described (28). Briefly, primary bone marrow cells were harvested from C57BL/6 or *Cxcr*$2^{-/-}$ mice and were resuspended after washing. Contaminating monocytes were depleted by adherence (30 min at 37°C). Cell suspensions (1×10^6 cells/well) were added onto the insert and the conditioned medium was added to the lower well. As a positive control, a recombinant CXCL2 (R&D Systems, Minneapolis, MN) was used. The conditioned medium from the NTHi-unexposed RSL cells was used as a negative control. Cells were allowed to migrate for 6 to 18 h at 37°C. After cytospin preparation and Giemsa staining, migrated PMNs were identified. Migrated cells were counted using a hemocytometer, and a fold-change was determined after normalization with the group of the conditioned medium from the NTHi-unexposed RSL cells.

ELISA

CXCL2 protein levels in the conditioned medium from the RSL cells were measured using rat CXCL2 ELISA kits (RayBiotech, Inc., Norcross, GA) following the manufacturer's instructions.

Quantitative RT-PCR

Quantitative RT-PCR was performed as described previously (27). Briefly, the RSL cells were exposed to the NTHi lysate, and total RNA was extracted using TRIzol reagent (Invitrogen). After cDNA was synthesized using the TaqMan® reverse transcription kit (Applied Biosystems), multiplex PCR was performed using the ABI 7500 Real-Time PCR system (Applied Biosystems) with gene-specific primers (FAM-conjugated probes for CXCL2) and control primers (a VIC-conjugated probe for GAPDH). The cycle threshold (C_T) values were determined according to the manufacturer's instructions, and the relative quantity of mRNA was determined using the $2^{-\Delta\Delta CT}$ method (39). C_T values were normalized to the internal control (GAPDH), and the results were expressed as a fold change of mRNA with the mRNA levels in the non-treated group set as 1.

Plasmids, transfections and luciferase assays

The vectors expressing a dominant-negative construct of MEK1 (K97R), a wild type construct of MEK1, a dominant-negative construct of ERK1 (K71R), a dominant-negative construct of ERK2 (T183A/Y185F) and a dominant-negative construct of c-Jun (TAM67) were previously described (40-43). Promoter fragments (-3475 to +14, -563 to +14, and -134 to +14) of the rat CXCL2 (NM_053647) were amplified, and *Kpn* I and *Xho*I sites were added with the following primers: 5'-AGGTACCTTTGCCCACTGGCAAGCCTACCAAGGCCTCTAC-3' (-3475); 5'-CGGGTACCAGGATATGACACAAAA-3' (-563); 5'-CGGTACCTACTCAGCTCTCGGGG-3' (-134); and 5'-GCTCGAGGGGCCATGGCGCT-3' (+14). Each fragment was ligated into *Kpn* I and *Xho* I sites of the pGL3 luciferase reporter plasmid (Promega, Madison, WI), and constructs were verified by sequencing. The luciferase-expressing constructs containing the promoter region

of the mouse CXCL2 (NM_009140) were provided by Dr. Hyung-Joo Kwon (Hallym University, Korea) (32). Constructs were transfected to cells using the Transit®-LT1 transfection reagent (Mirus, Madison, WI) according to the manufacturer's instructions. The pRL-TK vector (Promega) was cotransfected to normalize transfection efficiency. Transfected cells were then starved overnight in serum-free DMEM, followed by exposure to the NTHi lysate for 8 h before harvesting. All transfections were carried out in triplicate. After washing with PBS, cells were dissolved in the lysis reagent (Promega). Luciferase activity was measured using a luminometer (Pharmingen) after adding the necessary luciferase substrate (Promega). Results were expressed as a fold change of luciferase activity, taking the value of the non-treated group as 1.

Site-directed mutagenesis

To introduce site-specific mutations to the AP-1 motifs in the 5'-flanking region of the rat CXCL2, site-directed mutagenesis was performed with the QuikChange II XL Site-Directed Mutagenesis Kit (Agilent Technologies, Santa Clara, CA). Briefly, PCR was conducted to replicate mutagenic plasmids using the following primers: 5'-CCTTAATTTCTCCAGTCCTAATG**GTACC**AGTTCCTCAAACTGTTG-3' for the distal AP-1 motif and 5'-GAAGGGCAGGGAAGTATGATG**GGTACC**GCAGTTCATGCGTGCACG-3' for the proximal AP-1 motif. To completely digest parental template plasmids, 10 U of a methylation-sensitive restriction enzyme, *Dpn* I, was added to the PCR products and incubated overnight at 37°C. The mutated plasmids were transformed into *E. coli* XL10-Gold and the transformation mixture was plated on LB medium containing ampicillin. After preparation of plasmids, point mutations were identified with sequencing.

Phosphorylation assays

Cells were grown to 80% confluence in six-well culture plates. After overnight starvation with basal medium, cells were treated with the NTHi lysate for 3, 5, 10, 20, 40, and 60 min. Cells were lysed with cell lysis buffer (Cell Signaling Technology, Danvers, MA) supplemented with a protease inhibitor cocktail and 1 mM PMSF (Calbiochem). The lysates were then centrifuged at 14,000 × *g* for 15 min, and the supernatants were collected. For c-Jun, the nuclear proteins were collected using Nuclear Extract Kit (Active Motif) according to the manufacturer's instructions. After measurement of protein concentrations of supernatants, an amount equivalent to 20 μg of proteins was loaded onto 10% Tricine gels (Invitrogen), and electrophoresis was conducted in a Tris-Tricine-sodium dodecyl sulfate tank buffer (pH 7.4). After electrophoresis, proteins were transferred onto PVDF membranes (Bio-Rad, Hercules, CA) and washed three times for 5 min each in Tris-buffered saline plus 0.05% Tween 20 (TBST). Membranes were blocked using 5% nonfat dry milk in TBST for 1 h at room temperature and incubated overnight at 4°C in the presence of a 1:1,000 dilution of a polyclonal antibody against phosphorylated ERK1/2 and c-Jun, and total ERK1/2 and c-Jun (Cell Signaling Technology). After washing, membranes were incubated with a HRP-conjugated secondary antibody in a blocking buffer. Membranes were then incubated with a SuperSignal substrate (Pierce Biotechnologies) for 1 min at room temperature, and chemiluminescence signals were detected by exposure to X-ray films.

Transcription factor assays

NTHi-activated transcription factors were analyzed using the ELISA-based TransAM kit (Active Motif, Carlsbad, CA) as described (27). In brief, after the nuclear proteins were extracted from the RSL cells using Nuclear Extract Kit (Active Motif), nuclear proteins were applied to a 96-well plate coated with oligonucleotides containing the consensus sequences of various transcription factors. To demonstrate a binding specificity, binding activities oftranscription factors were inhibited with a competitor, unbound consensus

oligonucleotides. After washing, bound transcription factors were labeled with a 1:1,000 dilution ofprimary polyclonal antibodies against each transcription factor at room temperature for 1 h. Unbound antibodies were washed out, and wells were incubated with a 1:1,000 dilution of anti-rabbit IgG conjugated with HRP at room temperature for 30 min. 100 μl of tetramethylbenzidine substrate was added to each well and incubated at room temperature for 10 min. The absorbance was measured at 450 nm with a microplate reader.

Chromation immunoprecipitation

The RSL cells were treated with the NTHi lysate in the presence or absence of MEK inhibitor and fixed with 1% formaldehyde for 10 min. After lysis of cells with 1 ml of an ice-cold lysis buffer supplemented with a protease inhibitor cocktail and PMSF, the nuclear fraction was collected using Nuclear Extract Kit (Active Motif). After resuspending of the nuclear extract, enzymatic shearing of chromatins was conducted. The sheared DNA samples were centrifuged at 15,000 × *g* for 10 min at 4°C and the supernatant was collected (Input DNA). Input DNA samples were incubated with 3 μg/ml of an anti-phosphorylated c-Jun antibody and 25 μl of protein G magnetic beads for overnight at 4°C. The samples were placed on the magnetic stand to pellet beads and the supernatant was discarded carefully. After washing, the pelleted beads were resuspended and named as “ChIP DNA”. To reverse cross-links, ChIP DNA samples and Input DNA samples were incubated at 65°C for 2.5 h and then were mixed with 1 μg/μl of proteinase K and incubated at 37°C for 1 h. Conventional PCR and quantitative PCR was performed on Input DNA and ChIP DNA samples using the following primer pairs: 5’-TATGTAACTAACGGAGACGCACCC-3’ and 5’-AAACCCTCAGGAGGAAGGAAGTGA-3’ (Distal AP-1 motif, 190 bp); and 5’-TTGTCTGCCCTGATGACATCGCT-3’ and 5’-TTAGGGTCCCTGCATCAGGAAGAA-3’ (Proximal AP-1 motif, 230 bp).

Alternating laser excitation (ALEX) fluorescence spectroscopy

Alexa 647N-labeled 21-mer double stranded oligonucleotides containing the proximal and distal AP-1 motifs of the rat CXCL2 were prepared (IDT, Coralville, IA). The RSL cells were treated with NTHi lysate and lysed with cell lysis buffer. After extraction of nuclear fractions, samples were purified using Microcon (Ambion, Foster City, CA) to remove detergents and salts. Samples were resuspended in a Tris buffer (pH 7.5) and were incubated with Alexa 647N-labeled oligonucleotides overnight at 4°C (an acceptor). Samples were washed and incubated with an Alexa 488-labeled antibody against phosphorylated-c-Jun (Cell Signaling Technology) overnight at 4°C (a donor). In collaboration with Nesher Technologies, Inc. (Los Angeles, CA), ALEX fluorescence spectroscopy was performed as previously described (44-46). Briefly, the donor was directly excited by the first laser (488 nm), and the acceptor-derived emission (669 nm) was detected with and without the second laser (647 nm). Donor-acceptor stoichiometry was analyzed with normalization of burst counts by total burst counts of the consistent areas on the FRET efficiency and stoichiometry diagram.

Statistics

All experiments were carried out in triplicate and repeated twice. Results were expressed as means ± standard deviations. Statistical analysis was performed using Student's *t*-test and ANOVA followed by Tukey's post hoc test using the R2.14.0 software for Window (The R Foundation for Statistical Computing). A value of $p < 0.05$ was considered significant.

Results

SLFs up-regulate CXCL2 in response to NTHi-induced middle ear infection

In the prior study, we have demonstrated that the SLFs release MCP-1/CCL2 in response to NTHi, resulting in cochlear recruitment of monocytes (28). In addition to monocytes, our animal model for OM-induced inner ear inflammation showed that transtympanic inoculation of live NTHi leads to cochlear infiltration of PMNs (Supplemental Fig. 1*A*). Based on the finding that the SLFs are able to release various cytokines and chemokines in response to pro-inflammatory signals (13), we sought to determine if NTHi-induced SLF-derived molecules attract PMNs. As shown in Fig. 1*A*, the SLFs appeared to release CXCR2 ligands resulting in migration of PMNs. Among the CXCR2 ligands, we focused on CXCL2 since we found that the SLFs up-regulate CXCL2 in response to NTHi in the rats and mice (14) (Supplemental Fig. 1*C*). Next, we performed ELISA analysis to show NTHi-induced regulation of CXCL2 at the protein levels. In consistence with our previous findings (14), the RSL cells were found to up-regulate CXCL2 upon exposure to NTHi in a dose-dependent manner (Fig. 1*B*). To determine if CXCL2 is associated with OM-induced inner ear inflammation in vivo, immunolabeling of the murine temporal bone was performed using an anti-CXCL2 antibody after transtympanic inoculation of live NTHi. As shown in Fig. 1*C*, CXCL2 was highly expressed in the spiral ligament of the NTHi-inoculated mice, compared to the saline-inoculated mice. Transtympanic inoculation of NTHi was found to induce middle ear inflammation with mucosal thickening, which was resolved within seven days (data not shown). OM-induced inner ear inflammation was noted 5 to 6 days after NTHi inoculation and remained after resolution of middle ear inflammation, indicating that inner ear inflammation is secondary to OM. Taken together, it is suggested that the SLFs are critically involved in cochlear infiltration of PMNs secondary to NTHi-induced OM.

Activation of the c-Jun is required for NTHi-induced CXCL2 up-regulation

Based on the requirement of NF-κB for NTHi-induced up-regulation of MCP-1/CCL2 in the SLFs (27) and LPS-induced CXCL2 up-regulation in the murine macrophages (32, 33), we predicted that NF-κB is also involved in CXCL2 induction in response to NTHi. Unexpectedly, qRT-PCR analysis and ELISAs showed that inhibition of NF-κB signaling insignificantly suppresses NTHi-induced CXCL2 up-regulation in the RSL cells (Supplemental Fig. 2), suggesting the involvement of NF-κB-independent signaling pathways. Since transcriptional regulation of CXCL2 is known to vary according to the pro-inflammatory signals (32, 33, 47), we sought to explore transcription factors involved in NTHi-induced CXCL2 up-regulation using transcription factor ELISAs. The RSL cells were found to activate c-Jun in response to NTHi, leading to selective binding to the consensus sequences of AP-1 motifs (Fig. 2*A*). Moreover, phosphorylation assays showed NTHi-induced phosphorylation of nuclear c-Jun (Fig. 2*B*). We next sought to determine if NTHi-induced c-Jun activation requires NTHi-induced CXCL2 up-regulation. As shown in Fig. 2*C*, Tanshinone IIA, a c-Jun phosphorylation inhibitor, appeared to suppress NTHi-induced CXCL2 up-regulation in a dose-dependent manner. To further determine the involvement of c-Jun, luciferase assays were performed using a luciferase-expressing reporter containing the 5'-flanking region of the rat CXCL2 after the RSL cells were co-transfected with the dominant-negative construct of c-Jun (TAM67). As shown in Fig. 2*D*, NTHi-induced up-regulation of CXCL2 transcription was inhibited by TAM67. Consistently, ELISA analysis showed that TAM67 markedly suppresses NTHi-induced up-regulation of CXCL2 translation (Fig. 2*E*), suggesting that the activation of the c-Jun is required for NTHi-induced CXCL2 up-regulation.

MEK1-ERK2 signaling pathway is involved in NTHi-induced CXCL2 up-regulation in SLFs

To determine upstream signaling molecules involved in NTHi-induced c-Jun-mediated CXCL2 up-regulation, RSL cells were pretreated with chemical inhibitors of the MAP kinases. Interestingly, NTHi-induced CXCL2 up-regulation was markedly inhibited only by PD98059, but not by other MAPK inhibitors (Fig. 3*A*). To further investigate the involvement of MEK1, the RSL cells were transfected with a dominant-negative construct of MEK1. In consistence with the inhibitor study, a dominant-negative inhibition of MEK1 appeared to suppress NTHi-induced CXCL2 up-regulation. In contrast, over-expression of a wild type MEK1 enhanced NTHi-induced CXCL2 up-regulation (Fig. 3*B*). Since ERKs are downstream molecules of MEK1, we sought to determine the involvement of ERK1/2 in NTHi-induced CXCL2 up-regulation. As expected, pretreatment with AG126 (an MEK inhibitor) and FR180204 (an ERK inhibitor) significantly inhibited NTHi-induced CXCL2 up-regulation (Fig. 3*C*). Next, we performed phosphorylation assays to determine NTHi-induced ERK activation. Interestingly, only ERK2, not ERK1, was phosphorylated upon exposure to NTHi, peaking 10 min later (Fig. 3*D*). To further dissect functions of each ERK isoform, ERK expression was suppressed by a dominant-negative construct of ERK1 or ERK2. In consistence with the finding of the phosphorylation assays, NTHi-induced CXCL2 up-regulation was found to be inhibited only by a dominant-negative construct of ERK2, but not by ERK1 (Fig. 3*E*). Consistently, ELISA analysis showed that a dominant-negative inhibition of ERK2 markedly suppresses NTHi-induced CXCL2 up-regulation (Fig. 3*F*). Next, we sought to determine if NTHi-induced c-Jun activation requires the MEK-dependent signaling pathway. As shown in Fig. 3*G*, MEK inhibitors such as PD98059 and AG126 appeared to suppress NTHi-induced activation of c-Jun. These results suggested that MEK1/ERK2-mediated activation of c-Jun is involved in NTHi-induced CXCL2 up-regulation in the SLFs.

Identification of a NTHi-responsive AP-1 motif of CXCL2

To determine NTHi-responsive elements in the 5'-flanking region of CXCL2, the luciferase-expressing constructs containing the nested deletions of the 5'-flanking region of the rat CXCL2 were generated. Luciferase assays showed that the 134 bp-sized construct has the least promoter activity compared to the 3475 bp- and 563 bp-sized constructs (Fig. 4*A*), indicating that the NTHi-responsive elements exist between -563 bp and -134 bp of the 5'-flanking region of the rat CXCL2. The motif analysis of this region predicted two AP-1 motifs, which agreed with the previous studies showing that two AP-1 motifs exist in the 5'-flanking region of the mouse CXCL2 (32). To determine the requirement of these AP-1 motifs for NTHi-induced CXCL2 up-regulation in the SLFs, we conducted site-directed mutagenesis. As shown in Fig. 4*B*, NTHi-induced CXCL2 up-regulation was inhibited by the mutation of each AP-1 motif, and the mutation of both sites completely inhibited CXCL2 induction. Interestingly, the proximal AP-1 motif appeared to be more involved in NTHi-induced CXCL2 up-regulation than the distal one. In the mouse CXCL2, both AP-1 motifs were also found to be involved in NTHi-induced up-regulation of CXCL2 expression (Supplemental Fig. 3).

NTHi-activated c-Jun binds the AP-1 motif of CXCL2

Next, we sought to determine if NTHi-activated c-Jun binds the AP-1 motifs of the rat CXCL2. We performed ChIP-PCR assays using an anti-c-Jun antibody and the primers spanning either distal or proximal AP-1 motif of CXCL2. NTHi-activated c-Jun was found to bind both distal and proximal AP-1 motifs of the rat CXCL2 (Fig. 5*A*). We further investigated if the MEK-dependent signaling pathway is involved in NTHi-induced binding of c-Jun to both AP-1 motifs of the rat CXCL2. As shown Fig. 5*B*, PD98059 significantly inhibited NTHi-induced binding of c-Jun to both distal and proximal AP-1 motifs of CXCL2. Alignment analysis showed that three bases of the 3' side are different between the

proximal and distal AP-1 motifs (Fig. 6*A*). In addition, two AP-1 motifs were found to have only two bases in common out of 7 bases flanking the core recognition site in each side. To determine if this sequence difference leads to a difference in the binding affinity of the AP-1 motifs to NTHi-activated c-Jun in vitro, ALEX fluorescence spectroscopy was performed using the Alexa 647N-labeled DNA fragments containing each AP-1 motif and the Alexa 488-labeled antibody against c-Jun. Interestingly, only the proximal AP-1 motif, not the distal one, showed 2.13 ± 0.53-fold increase in ALEX efficiency (Fig. 6*B*). This result indicated that the proximal AP-1 motif has a higher binding affinity to NTHi-activated c-Jun than the distal one in vitro, agreeing with our site-directed mutagenesis study. Taken together, it is suggested that MEK-dependent activation of c-Jun is required for NTHi-induced binding of c-Jun to the proximal AP-1 binding motif of CXCL2, resulting in up-regulation of CXCL2 expression.

Discussion

In this study, we showed that the SLFs up-regulate CXCL2 in response to NTHi via ERK2-dependent activation of the c-Jun, which is involved in inner ear inflammation secondary to OM. We also found that binding of c-Jun to the AP-1 motifs, particularly to the proximal one, in the 5'-flanking region of CXCL2 is required for NTHi-induced CXCL2 up-regulation. Furthermore, we demonstrated a higher binding affinity of the proximal AP-1 motif to NTHi-activated c-Jun.

PMNs are a major element of the innate immune defense against invading pathogens, but their overly-robust response can lead to pathological sequelae from local tissue damage to organ dysfunction. Since OM-induced cochlear infiltration of PMNs is believed to contribute OM-induced SNHL (48), it is important to understand the molecular mechanism involved in the cochlear infiltration of PMNs in response to middle ear inflammation. In this study, we showed that fibrocytes of the cochlear spiral ligament release PMN-attracting CXCR2 ligands in response to NTHi. In humans, IL-8 (CXCL8) is a major PMN chemoattractive agent (49-51), whereas CXCL1 and CXCL2 are known to mainly serve as CXCR2 ligands leading to chemoattraction of PMNs in rodents. Although the RSL cells are suggested to release a variety of PMN-attracting molecules in response to NTHi (Supplemental Fig. 1*B*), we further focused on CXCL2 regulation based on the findings that CXCL2 is more active than CXCL1 in recruiting PMNs (52-54).

CXCL2 was first identified as a major heparin-binding protein secreted from the endotoxin-stimulated murine macrophages (55). Besides a potent chemoattractive activity for PMNs, animal experiments showed the role of CXCL2 in regulation of ischemia-induced leukocyte adhesion (56) and sepsis-mediated lung injury (57). Furthermore, CXCL2 was found to be involved in proliferation and protection of hepatocytes (58, 59), pulmonary angiogenesis and fibrosis (60), osteoclastogenesis (61), hepatic metastasis of colorectal cancer cells (62), and stem cell mobilization (63) in the animal studies. In humans, CXCL2 was discovered as one of the GRO genes having a growth-stimulating activity (64). CXCL2 is clinically a potential cancer marker since CXCL2 dysregulation is frequently found in patients with esophageal carcinoma (65), non-small cell lung cancer (66) and colon cancer (67). In addition, a CXCL2 polymorphism is known to be associated with higher mortality of sepsis (68). The role of CXCL2 in inner ear inflammation is poorly understood, but we here demonstrated the molecular mechanism involved in contribution of SLF-derived CXCL2 to OM-induced inner ear inflammation.

Transcription of CXCL2 is known to be regulated by the NF-κB- and/or c-Jun-dependent signaling. LPS induces CXCL2 via both NF-κB and c-Jun-dependent regulation in the mouse macrophage cell line (32), whereas pyrrolidine dithiocarbomate-induced CXCL2 up-

regulation is NF-κB-independent but c-Jun-dependent (33). In addition, oligodeoxynucleotide containing CpG motif is known to up-regulate CXCL2 only via NF-κB activation (47). Unlike other gram-negative bacteria, NTHi contains atypical LPS, i.e. lipooligosaccharides lacking an O-specific polysaccharide in the outer membrane (69). In contrast to LPS, this study showed that NTHi up-regulates CXCL2 only via c-Jun activation mediated by ERK2 phosphorylation.

The AP-1 complex, a dimer of Jun, Fos, and ATF family members binding AP-1 motifs, is involved in activation of genes associated with various cellular events such as proliferation, differentiation and apoptosis (70, 71). A heterodimer of c-Jun and c-Fos is known to most frequently serve as an AP-1 complex (72). c-Jun can form a homodimer, whereas Fos proteins usually do not form a homodimer (73). In agreement with our previous report showing that c-Fos is not highly activated in response to NTHi (27), a dominant-negative construct of c-Fos (A-Fos) did not inhibit the NTHi-induced CXCL2 up-regulation (data not shown). These results suggest that the NTHi-activated AP-1 complex is either a c-Jun homodimer or a c-Jun heterodimer with other AP-1 components than c-Fos. Generally, c-Jun is known to be activated by a Jun N-terminal kinase (JNK)-mediated signaling pathway. However, our results showed ERK2, not JNK, is critically involved in NTHi-induced CXCL2 up-regulation. In agreement with our result, *Helicobacter pylori* induces apoptosis in macrophages via ERK-dependent activation of c-Jun (71). In addition, ERK-dependent c-Jun activation is known to induce neuronal differentiation, while JNK-mediated c-Jun activation is involved in induction of apoptosis (74), suggesting that the upstream molecules involved in c-Jun activation affect c-Jun-mediated cellular events.

Furthermore, we found that ERK2, not ERK1, is strongly involved in NTHi-induced CXCL2 up-regulation in the SLFs. Specific functions of each ERK isoform remain unclear, but functional redundancy has been a working model since ERK isoforms are 90% identical to each other (75) and share activators and substrates. However, there is emerging evidence showing that ERK1 and ERK2 have different functions. Deficiency of ERK2 results in early embryonic death due to a placental defect (76), but the lack of ERK1 does not influence growth and reproduction of mice (77). Silencing of ERK2 appeared to completely suppress cell proliferation, while ERK1 deficiency resulted in a growth advantage associated with an enhancement of ERK2-dependent signaling (78). ERK is known to be required for NTHi-induced IL-8 production in the human epithelial cells (79), but only one of the ERK isoforms was noted to be phosphorylated upon exposure to NTHi. Our study indicates that NTHi-activated ERK isoform is ERK2 resulting in CXCL2 induction, which will bring a new insight into a novel role of the ERK2 isoform in bacterial infections.

TLR2 is known to play an important role in recognition of NTHi molecules in epithelial cells (80). We also demonstrated that the SLFs up-regulate MCP-1/CCL2 in response to NTHi via TLR2/MyD88 signaling (27). Consistently, we found that TLR2 and MyD88 are involved in NTHi-induced CXCL2 up-regulation in the SLFs (Supplemental Fig. 4). This result suggests that ERK signaling mediates NTHi-induced TLR2 signaling although NTHi-induced TLR2 signaling is known to be transmitted mainly through p38 MAP kinases (81-83). Similarly, TLR2-dependent ERK activation has been reported to be involved in bacterial teichoic acid-induced up-regulation of IL-10 (84) and iNOS (85), and hepatitis C virus-induced neurotoxic effects (86). Moreover, transient hypoxia of the kidney cells is known to induce TLR2-mediated activation of ERK (87).

Although ChIP analysis showed that NTHi-activated c-Jun binds both distal and proximal AP-1 motifs of CXCL2, ALEX fluorescence spectroscopy demonstrated that the proximal AP-1 motif has a higher binding affinity to NTHi-activated c-Jun than the distal one. Consistent with the finding of ALEX fluorescence spectroscopy, site-directed mutagenesis

revealed that the proximal AP-1 motif contributes to NTHi-induced CXCL2 up-regulation more than the distal one. The AP-1 motif is asymmetric from the central C:G base pair, but binding of AP-1 is orientation-independent (88). Sequences flanking the conserved AP-1 core recognition site also affect the affinity of AP-1 binding (89, 90) through influencing of DNA bending (91). Difference in core recognition sequences and flanking sequences of two AP-1 motifs of CXCL2 may contribute to difference in the binding affinity of two AP-1 motifs, but further studies are needed to reveal a key sequence involved in a higher binding affinity of the proximal one.

In conclusion, we demonstrated that the SLFs play a central role in inner ear inflammation by up-regulation of CXCL2 through c-Jun activation mediated by a MEK1/ERK2-dependent signaling pathway. SLF-derived CXCL2 is suggested to recruit PMNs to the cochlea, and inflammation-associated tissue damage is believed to contribute to OM-induced inner ear dysfunction such as sensorineural hearing loss. Our study will bring an insight into the molecular pathogenesis of OM-induced inner ear dysfunction and provide a novel strategy for the prevention of inner ear complication secondary to middle ear inflammation.

Supplementary Material

Refer to Web version on PubMed Central for supplementary material.

Acknowledgments

We would like to thank Drs. Nancy Colburn (NCI, NIH), Jian-Dong Li (Georgia State University) and Hyung-Joo Kwon (Hallym University, Korea) for providing the constructs used in this study, and Dr. Seok Won Yim (Nesher Technologies, Inc.) for providing the technical support of ALEX fluorescence spectroscopy. We also thank Dr. Laurel Fisher (House Research Institute) for statistical analysis and Yoo Jin Lee (House Research Institute) for technical assistance.

This work was supported in part by grants DC8696, DC5025 and DC6276 from National Institutes of Health, National Institute Deafness and Other Communication Disorders.

Abbreviations used in this paper

ALEX	alternating laser excitation fluorescence spectroscopy
ChIP	chromatin immunoprecipitation
NTHi	nontypeable *Haemphilus influenzae*
OM	otitis media
RSL	rat spiral ligament cell line
SLF	spiral ligament fibrocyte
SNHL	sensorineural hearing loss

References

1. Lim DJ. Functional structure of the organ of Corti: a review. Hear. Res. 1986; 22:117–146. [PubMed: 3525482]
2. Lim DJ. Vestibular sensory organs. A scanning electron microscopic investigation. Arch. Otolaryngol. 1971; 94:69–76. [PubMed: 5555875]
3. Juhn SK. Barrier systems in the inner ear. Acta Otolaryngol. Suppl. 1988; 458:79–83. [PubMed: 3245438]
4. Harris JP, Ryan AF. Fundamental immune mechanisms of the brain and inner ear. Otolaryngol. Head Neck Surg. 1995; 112:639–653. [PubMed: 7777346]

5. Okano T, Nakagawa T, Kita T, Kada S, Yoshimoto M, Nakahata T, Ito J. Bone marrow-derived cells expressing Iba1 are constitutively present as resident tissue macrophages in the mouse cochlea. J. Neurosci. Res. 2008; 86:1758–1767. [PubMed: 18253944]
6. Hashimoto S, Billings P, Harris JP, Firestein GS, Keithley EM. Innate immunity contributes to cochlear adaptive immune responses. Audiol. Neurootol. 2005; 10:35–43. [PubMed: 15567913]
7. Adams JC, Seed B, Lu N, Landry A, Xavier RJ. Selective activation of nuclear factor kappa B in the cochlea by sensory and inflammatory stress. Neuroscience. 2009; 160:530–539. [PubMed: 19285117]
8. Lecain E, Sauvaget E, Crisanti P, Van Den Abbeele T, Huy PT. Potassium channel ether a go-go mRNA expression in the spiral ligament of the rat. Hear. Res. 1999; 133:133–138. [PubMed: 10416871]
9. Lautermann J, ten Cate WJ, Altenhoff P, Grummer R, Traub O, Frank H, Jahnke K, Winterhager E. Expression of the gap-junction connexins 26 and 30 in the rat cochlea. Cell Tissue Res. 1998; 294:415–420. [PubMed: 9799458]
10. Crouch JJ, Sakaguchi N, Lytle C, Schulte BA. Immunohistochemical localization of the Na-K-Cl co-transporter (NKCC1) in the gerbil inner ear. J. Histochem. Cytochem. 1997; 45:773–778. [PubMed: 9199662]
11. Qu C, Liang F, Hu W, Shen Z, Spicer SS, Schulte BA. Expression of CLC-K chloride channels in the rat cochlea. Hear. Res. 2006; 213:79–87. [PubMed: 16466872]
12. Spicer SS, Schulte BA. Differentiation of inner ear fibrocytes according to their ion transport related activity. Hear. Res. 1991; 56:53–64. [PubMed: 1663106]
13. Yoshida K, Ichimiya I, Suzuki M, Mogi G. Effect of proinflammatory cytokines on cultured spiral ligament fibrocytes. Hear. Res. 1999; 137:155–159. [PubMed: 10545642]
14. Moon SK, Park R, Lee HY, Nam GJ, Cha K, Andalibi A, Lim DJ. Spiral ligament fibrocytes release chemokines in response to otitis media pathogens. Acta Otolaryngol. 2006; 126:564–569. [PubMed: 16720438]
15. Bernius M, Perlin D. Pediatric ear, nose, and throat emergencies. Pediatr. Clin. North Am. 2006; 53:195–214. [PubMed: 16574522]
16. Paparella MM, Goycoolea MV, Meyerhoff WL. Inner ear pathology and otitis media. A review. Ann. Otol. Rhinol. Laryngol. Suppl. 1980; 89:249–253. [PubMed: 6778318]
17. Paparella MM, Morizono T, Le CT, Mancini F, Sipila P, Choo YB, Liden G, Kim CS. Sensorineural hearing loss in otitis media. Ann. Otol. Rhinol. Laryngol. 1984; 93:623–629. [PubMed: 6508134]
18. Casselbrant ML, Furman JM, Rubenstein E, Mandel EM. Effect of otitis media on the vestibular system in children. Ann. Otol. Rhinol. Laryngol. 1995; 104:620–624. [PubMed: 7639471]
19. Bess FH, Dodd-Murphy J, Parker RA. Children with minimal sensorineural hearing loss: prevalence, educational performance, and functional status. Ear. Hear. 1998; 19:339–354. [PubMed: 9796643]
20. Casselbrant ML, Villardo RJ, Mandel EM. Balance and otitis media with effusion. Int. J. Audiol. 2008; 47:584–589. [PubMed: 18821228]
21. Hunter LL, Margolis RH, Rykken JR, Le CT, Daly KA, Giebink GS. High frequency hearing loss associated with otitis media. Ear. Hear. 1996; 17:1–11. [PubMed: 8741962]
22. Mutlu C, Odabasi AO, Metin K, Basak S, Erpek G. Sensorineural hearing loss associated with otitis media with effusion in children. Int. J. Pediatr. Otorhinolaryngol. 1998; 46:179–184. [PubMed: 10190588]
23. Kawauchi H, DeMaria TF, Lim DJ. Endotoxin permeability through the round window. Acta Otolaryngol. Suppl. 1989; 457:100–115. [PubMed: 2648753]
24. Cook RD, Postma DS, Brinson GM, Prazma J, Pillsbury HC. Cytotoxic changes in hair cells secondary to pneumococcal middle-ear infection. J. Otolaryngol. 1999; 28:325–331. [PubMed: 10604161]
25. Ichimiya I, Suzuki M, Hirano T, Mogi G. The influence of pneumococcal otitis media on the cochlear lateral wall. Hear. Res. 1999; 131:128–134. [PubMed: 10355610]

26. Tsuprun V, Cureoglu S, Schachern PA, Ferrieri P, Briles DE, Paparella MM, Juhn SK. Role of pneumococcal proteins in sensorineural hearing loss due to otitis media. Otol. Neurotol. 2008; 29:1056–1060. [PubMed: 18833010]
27. Moon SK, Woo JI, Lee HY, Park R, Shimada J, Pan H, Gellibolian R, Lim DJ. Toll-like receptor 2-dependent NF-kappaB activation is involved in nontypeable Haemophilus influenzae-induced monocyte chemotactic protein 1 up-regulation in the spiral ligament fibrocytes of the inner ear. Infect. Immun. 2007; 75:3361–3372. [PubMed: 17452470]
28. Woo JI, Pan H, Oh S, Lim DJ, Moon SK. Spiral ligament fibrocyte-derived MCP-1/CCL2 contributes to inner ear inflammation secondary to nontypeable H. influenzae-induced otitis media. BMC Infect. Dis. 2010; 10:314. [PubMed: 21029462]
29. Feng L, Xia Y, Yoshimura T, Wilson CB. Modulation of neutrophil influx in glomerulonephritis in the rat with anti-macrophage inflammatory protein-2 (MIP-2) antibody. J. Clin. Invest. 1995; 95:1009–1017. [PubMed: 7883948]
30. Schrier DJ, Schimmer RC, Flory CM, Tung DK, Ward PA. Role of chemokines and cytokines in a reactivation model of arthritis in rats induced by injection with streptococcal cell walls. J. Leukoc. Biol. 1998; 63:359–363. [PubMed: 9500524]
31. Skidgel RA, Gao XP, Brovkovych V, Rahman A, Jho D, Predescu S, Standiford TJ, Malik AB. Nitric oxide stimulates macrophage inflammatory protein-2 expression in sepsis. J. Immunol. 2002; 169:2093–2101. [PubMed: 12165537]
32. Kim DS, Han JH, Kwon HJ. NF-kappaB and c-Jun-dependent regulation of macrophage inflammatory protein-2 gene expression in response to lipopolysaccharide in RAW 264.7 cells. Mol. Immunol. 2003; 40:633–643. [PubMed: 14597166]
33. Sohn WJ, Lee KW, Lee Y, Han JH, Choe YK, Kim DS, Kwon HJ. Pyrrolidine dithiocarbamate-induced macrophage inflammatory protein-2 gene expression is NF-kappaB-independent but c-Jun-dependent in macrophage cell line RAW 264.7. Mol. Immunol. 2005; 42:1165–1175. [PubMed: 15829306]
34. Lee KW, Lee Y, Kwon HJ, Kim DS. Sp1-associated activation of macrophage inflammatory protein-2 promoter by CpG-oligodeoxynucleotide and lipopolysaccharide. Cell Mol. Life Sci. 2005; 62:188–198. [PubMed: 15666090]
35. Barenkamp SJ, Leininger E. Cloning, expression, and DNA sequence analysis of genes encoding nontypeable Haemophilus influenzae high-molecular-weight surface-exposed proteins related to filamentous hemagglutinin of Bordetella pertussis. Infect. Immun. 1992; 60:1302–1313. [PubMed: 1548058]
36. Moon SK, Lee HY, Pan H, Takeshita T, Park R, Cha K, Andalibi A, Lim DJ. Synergistic effect of interleukin 1 alpha on nontypeable Haemophilus influenzae-induced up-regulation of human beta-defensin 2 in middle ear epithelial cells. BMC Infect. Dis. 2006; 6:12. [PubMed: 16433908]
37. Yian C, Moon SK, Jin S, Webster P, Rhim JS, Andalibi A, Lim DJ. Characterization of rat spiral ligament cell line immortalized by adenovirus 12-simian virus 40 hybrid virus. Ann. Otol. Rhinol. Laryngol. 2006; 115:930–938. [PubMed: 17214269]
38. Suko T, Ichimiya I, Yoshida K, Suzuki M, Mogi G. Classification and culture of spiral ligament fibrocytes from mice. Hear. Res. 2000; 140:137–144. [PubMed: 10675641]
39. Livak KJ, Schmittgen TD. Analysis of relative gene expression data using real-time quantitative PCR and the 2(-Delta Delta C(T)) Method. Methods. 2001; 25:402–408. [PubMed: 11846609]
40. Moon SK, Lee HY, Li JD, Nagura M, Kang SH, Chun YM, Linthicum FH, Ganz T, Andalibi A, Lim DJ. Activation of a Src-dependent Raf-MEK1/2-ERK signaling pathway is required for IL-1alpha-induced upregulation of beta-defensin 2 in human middle ear epithelial cells. Biochim. Biophys. Acta. 2002; 1590:41–51. [PubMed: 12063167]
41. Kato Y, Kravchenko VV, Tapping RI, Han J, Ulevitch RJ, Lee JD. BMK1/ERK5 regulates serum-induced early gene expression through transcription factor MEF2C. EMBO J. 1997; 16:7054–7066. [PubMed: 9384584]
42. Robbins DJ, Zhen E, Owaki H, Vanderbilt CA, Ebert D, Geppert TD, Cobb MH. Regulation and properties of extracellular signal-regulated protein kinases 1 and 2 in vitro. J. Biol. Chem. 1993; 268:5097–5106. [PubMed: 8444886]

43. Young MR, Li JJ, Rincon M, Flavell RA, Sathyanarayana BK, Hunziker R, Colburn N. Transgenic mice demonstrate AP-1 (activator protein-1) transactivation is required for tumor promotion. Proc. Natl. Acad. Sci. USA. 1999; 96:9827–9832. [PubMed: 10449779]
44. Kapanidis AN, Lee NK, Laurence TA, Doose S, Margeat E, Weiss S. Fluorescence-aided molecule sorting: analysis of structure and interactions by alternating-laser excitation of single molecules. Proc. Natl. Acad. Sci. USA. 2004; 101:8936–8941. [PubMed: 15175430]
45. Lee NK, Kapanidis AN, Wang Y, Michalet X, Mukhopadhyay J, Ebright RH, Weiss S. Accurate FRET measurements within single diffusing biomolecules using alternating-laser excitation. Biophys. J. 2005; 88:2939–2953. [PubMed: 15653725]
46. Lee NK, Kapanidis AN, Koh HR, Korlann Y, Ho SO, Kim Y, Gassman N, Kim SK, Weiss S. Three-color alternating-laser excitation of single molecules: monitoring multiple interactions and distances. Biophys. J. 2007; 92:303–312. [PubMed: 17040983]
47. Kwon HJ, Kim DS. Regulation of macrophage inflammatory protein-2 gene expression in response to oligodeoxynucleotide containing CpG motifs in RAW 264.7 cells. Biochem. Biophys. Res. Commun. 2003; 308:608–613. [PubMed: 12914794]
48. Brandt CT, Caye-Thomasen P, Lund SP, Worsoe L, Ostergaard C, Frimodt-Moller N, Espersen F, Thomsen J, Lundgren JD. Hearing loss and cochlear damage in experimental pneumococcal meningitis, with special reference to the role of neutrophil granulocytes. Neurobiol. Dis. 2006; 23:300–311. [PubMed: 16798006]
49. Ina K, Kusugami K, Yamaguchi T, Imada A, Hosokawa T, Ohsuga M, Shinoda M, Ando T, Ito K, Yokoyama Y. Mucosal interleukin-8 is involved in neutrophil migration and binding to extracellular matrix in inflammatory bowel disease. Am. J. Gastroenterol. 1997; 92:1342–1346. [PubMed: 9260803]
50. Murphy PM. Neutrophil receptors for interleukin-8 and related CXC chemokines. Semin. Hematol. 1997; 34:311–318. [PubMed: 9347581]
51. Zimmermann HW, Seidler S, Gassler N, Nattermann J, Luedde T, Trautwein C, Tacke F. Interleukin-8 is activated in patients with chronic liver diseases and associated with hepatic macrophage accumulation in human liver fibrosis. PLoS One. 2010; 6:e21381. [PubMed: 21731723]
52. Frevert CW, Huang S, Danaee H, Paulauskis JD, Kobzik L. Functional characterization of the rat chemokine KC and its importance in neutrophil recruitment in a rat model of pulmonary inflammation. J. Immunol. 1995; 154:335–344. [PubMed: 7995953]
53. Tessier PA, Naccache PH, Clark-Lewis I, Gladue RP, Neote KS, McColl SR. Chemokine networks in vivo: involvement of C-X-C and C-C chemokines in neutrophil extravasation in vivo in response to TNF-alpha. J. Immunol. 1997; 159:3595–3602. [PubMed: 9317159]
54. Yan XT, Tumpey TM, Kunkel SL, Oakes JE, Lausch RN. Role of MIP-2 in neutrophil migration and tissue injury in the herpes simplex virus-1-infected cornea. Invest .Ophthalmol. Vis. Sci. 1998; 39:1854–1862. [PubMed: 9727408]
55. Wolpe SD, Cerami A. Macrophage inflammatory proteins 1 and 2: members of a novel superfamily of cytokines. FASEB J. 1989; 3:2565–2573. [PubMed: 2687068]
56. Riaz AA, Schramm R, Sato T, Menger MD, Jeppsson B, Thorlacius H. Oxygen radical-dependent expression of CXC chemokines regulate ischemia/reperfusion-induced leukocyte adhesion in the mouse colon. Free Radic. Biol. Med. 2003; 35:782–789. [PubMed: 14583342]
57. Kalyanaraman M, Heidemann SM, Sarnaik AP. Macrophage inflammatory protein-2 predicts acute lung injury in endotoxemia. J. Investig. Med. 1998; 46:275–278.
58. Li X, Klintman D, Liu Q, Sato T, Jeppsson B, Thorlacius H. Critical role of CXC chemokines in endotoxemic liver injury in mice. J. Leukoc. Biol. 2004; 75:443–452. [PubMed: 14673016]
59. Ren X, Carpenter A, Hogaboam C, Colletti L. Mitogenic properties of endogenous and pharmacological doses of macrophage inflammatory protein-2 after 70% hepatectomy in the mouse. Am. J. Pathol. 2003; 163:563–570. [PubMed: 12875976]
60. Keane MP, Belperio JA, Moore TA, Moore BB, Arenberg DA, Smith RE, Burdick MD, Kunkel SL, Strieter RM. Neutralization of the CXC chemokine, macrophage inflammatory protein-2, attenuates bleomycin-induced pulmonary fibrosis. J. Immunol. 1999; 162:5511–5518. [PubMed: 10228032]

61. Ha J, Choi HS, Lee Y, Kwon HJ, Song YW, Kim HH. CXC chemokine ligand 2 induced by receptor activator of NF-kappa B ligand enhances osteoclastogenesis. J. Immunol. 2010; 184:4717–4724. [PubMed: 20357249]
62. Kollmar O, Menger MD, Schilling MK. Macrophage inflammatory protein-2 contributes to liver resection-induced acceleration of hepatic metastatic tumor growth. World J. Gastroenterol. 2006; 12:858–867. [PubMed: 16521212]
63. Pelus LM, Fukuda S. Peripheral blood stem cell mobilization: the CXCR2 ligand GRObeta rapidly mobilizes hematopoietic stem cells with enhanced engraftment properties. Exp. Hematol. 2006; 34:1010–1020. [PubMed: 16863907]
64. Haskill S, Peace A, Morris J, Sporn SA, Anisowicz A, Lee SW, Smith T, Martin G, Ralph P, Sager R. Identification of three related human GRO genes encoding cytokine functions. Proc. Natl. Acad. Sci. USA. 1990; 87:7732–7736. [PubMed: 2217207]
65. Dong QM, Zhang JQ, Li Q, Bracher JC, Hendricks DT, Zhao XH. Clinical significance of serum expression of GRObeta in esophageal squamous cell carcinoma. World J. Gastroenterol. 2011; 17:2658–2662. [PubMed: 21677836]
66. Baird AM, Gray SG, O'Byrne KJ. Epigenetics underpinning the regulation of the CXC (ELR+) chemokines in non-small cell lung cancer. PLoS One. 2011; 6:e14593. [PubMed: 21298036]
67. Doll D, Keller L, Maak M, Boulesteix AL, Siewert JR, Holzmann B, Janssen KP. Differential expression of the chemokines GRO-2, GRO-3, and interleukin-8 in colon cancer and their impact on metastatic disease and survival. Int. J. Colorectal. Dis. 2010; 25:573–581. [PubMed: 20162422]
68. Villar J, Perez-Mendez L, Flores C, Maca-Meyer N, Espinosa E, Muriel A, Sanguesa R, Blanco J, Muros M, Kacmarek RM. A CXCL2 polymorphism is associated with better outcomes in patients with severe sepsis. Crit. Care Med. 2007; 35:2292–2297. [PubMed: 17944017]
69. Phillips NJ, Apicella MA, Griffiss JM, Gibson BW. Structural characterization of the cell surface lipooligosaccharides from a nontypable strain of Haemophilus influenzae. Biochemistry. 1992; 31:4515–4526. [PubMed: 1581306]
70. Herdegen T, Waetzig V. AP-1 proteins in the adult brain: facts and fiction about effectors of neuroprotection and neurodegeneration. Oncogene. 2001; 20:2424–2437. [PubMed: 11402338]
71. Asim M, Chaturvedi R, Hoge S, Lewis ND, Singh K, Barry DP, Algood HS, de Sablet T, Gobert AP, Wilson KT. Helicobacter pylori induces ERK-dependent formation of a phospho-c-Fos c-Jun activator protein-1 complex that causes apoptosis in macrophages. J. Biol. Chem. 2010; 285:20343–20357. [PubMed: 20410304]
72. Angel P, Karin M. The role of Jun, Fos and the AP-1 complex in cell-proliferation and transformation. Biochim. Biophys. Acta. 1991; 1072:129–157. [PubMed: 1751545]
73. Shaulian E, Karin M. AP-1 as a regulator of cell life and death. Nat. Cell Biol. 2002; 4:E131–136. [PubMed: 11988758]
74. Leppa S, Saffrich R, Ansorge W, Bohmann D. Differential regulation of c-Jun by ERK and JNK during PC12 cell differentiation. EMBO J. 1998; 17:4404–4413. [PubMed: 9687508]
75. Boulton TG, Gregory JS, Cobb MH. Purification and properties of extracellular signal-regulated kinase 1, an insulin-stimulated microtubule-associated protein 2 kinase. Biochemistry. 1991; 30:278–286. [PubMed: 1846291]
76. Yao Y, Li W, Wu J, Germann UA, Su MS, Kuida K, Boucher DM. Extracellular signal-regulated kinase 2 is necessary for mesoderm differentiation. Proc. Natl. Acad. Sci. USA. 2003; 100:12759–12764. [PubMed: 14566055]
77. Nekrasova T, Shive C, Gao Y, Kawamura K, Guardia R, Landreth G, Forsthuber TG. ERK1-deficient mice show normal T cell effector function and are highly susceptible to experimental autoimmune encephalomyelitis. J. Immunol. 2005; 175:2374–2380. [PubMed: 16081808]
78. Vantaggiato C, Formentini I, Bondanza A, Bonini C, Naldini L, Brambilla R. ERK1 and ERK2 mitogen-activated protein kinases affect Ras-dependent cell signaling differentially. J. Biol. 2006; 5:14. [PubMed: 16805921]
79. Wang B, Cleary PP, Xu H, Li JD. Up-regulation of interleukin-8 by novel small cytoplasmic molecules of nontypeable Haemophilus influenzae via p38 and extracellular signal-regulated kinase pathways. Infect. Immun. 2003; 71:5523–5530. [PubMed: 14500470]

80. Shuto T, Xu H, Wang B, Han J, Kai H, Gu XX, Murphy TF, Lim DJ, Li JD. Activation of NF-kappa B by nontypeable Hemophilus influenzae is mediated by toll-like receptor 2-TAK1-dependent NIK-IKK alpha /beta-I kappa B alpha and MKK3/6-p38 MAP kinase signaling pathways in epithelial cells. Proc. Natl. Acad. Sci. USA. 2001; 98:8774–8779. [PubMed: 11438700]
81. Wang B, Lim DJ, Han J, Kim YS, Basbaum CB, Li JD. Novel cytoplasmic proteins of nontypeable Haemophilus influenzae up-regulate human MUC5AC mucin transcription via a positive p38 mitogen-activated protein kinase pathway and a negative phosphoinositide 3-kinase-Akt pathway. J. Biol. Chem. 2002; 277:949–957. [PubMed: 11698399]
82. Jono H, Xu H, Kai H, Lim DJ, Kim YS, Feng XH, Li JD. Transforming growth factor-beta-Smad signaling pathway negatively regulates nontypeable Haemophilus influenzae-induced MUC5AC mucin transcription via mitogen-activated protein kinase (MAPK) phosphatase-1-dependent inhibition of p38 MAPK. J. Biol. Chem. 2003; 278:27811–27819. [PubMed: 12734193]
83. Lee HY, Takeshita T, Shimada J, Akopyan A, Woo JI, Pan H, Moon SK, Andalibi A, Park RK, Kang SH, Kang SS, Gellibolian R, Lim DJ. Induction of beta defensin 2 by NTHi requires TLR2 mediated MyD88 and IRAK-TRAF6-p38MAPK signaling pathway in human middle ear epithelial cells. BMC Infect. Dis. 2008; 8:87. [PubMed: 18578886]
84. Kaji R, Kiyoshima-Shibata J, Nagaoka M, Nanno M, Shida K. Bacterial teichoic acids reverse predominant IL-12 production induced by certain lactobacillus strains into predominant IL-10 production via TLR2-dependent ERK activation in macrophages. J. Immunol. 2010; 184:3505–3513. [PubMed: 20190136]
85. Chiu WT, Lin YL, Chou CW, Chen RM. Propofol inhibits lipoteichoic acid-induced iNOS gene expression in macrophages possibly through downregulation of toll-like receptor 2-mediated activation of Raf-MEK1/2-ERK1/2-IKK-NFkappaB. Chem. Biol. Interact. 2009; 181:430–439. [PubMed: 19573522]
86. Paulino AD, Ubhi K, Rockenstein E, Adame A, Crews L, Letendre S, Ellis R, Everall IP, Grant I, Masliah E. Neurotoxic effects of the HCV core protein are mediated by sustained activation of ERK via TLR2 signaling. J. Neurovirol. 2011; 17:327–340. [PubMed: 21660601]
87. Mkaddem SB, Werts C, Goujon JM, Bens M, Pedruzzi E, Ogier-Denis E, Vandewalle A. Heat shock protein gp96 interacts with protein phosphatase 5 and controls toll-like receptor 2 (TLR2)-mediated activation of extracellular signal-regulated kinase (ERK) 1/2 in post-hypoxic kidney cells. J. Biol. Chem. 2009; 284:12541–12549. [PubMed: 19265198]
88. Chen L, Oakley MG, Glover JN, Jain J, Dervan PB, Hogan PG, Rao A, Verdine GL. Only one of the two DNA-bound orientations of AP-1 found in solution cooperates with NFATp. Curr. Biol. 1995; 5:882–889. [PubMed: 7583146]
89. Ryseck RP, Bravo R. c-JUN, JUN B, and JUN D differ in their binding affinities to AP-1 and CRE consensus sequences: effect of FOS proteins. Oncogene. 1991; 6:533–542. [PubMed: 1827665]
90. Kerppola TK, Curran T. A conserved region adjacent to the basic domain is required for recognition of an extended DNA binding site by Maf/Nrl family proteins. Oncogene. 1994; 9:3149–3158. [PubMed: 7936637]
91. Rajaram N, Kerppola TK. DNA bending by Fos-Jun and the orientation of heterodimer binding depend on the sequence of the AP-1 site. EMBO J. 1997; 16:2917–2925. [PubMed: 9184235]

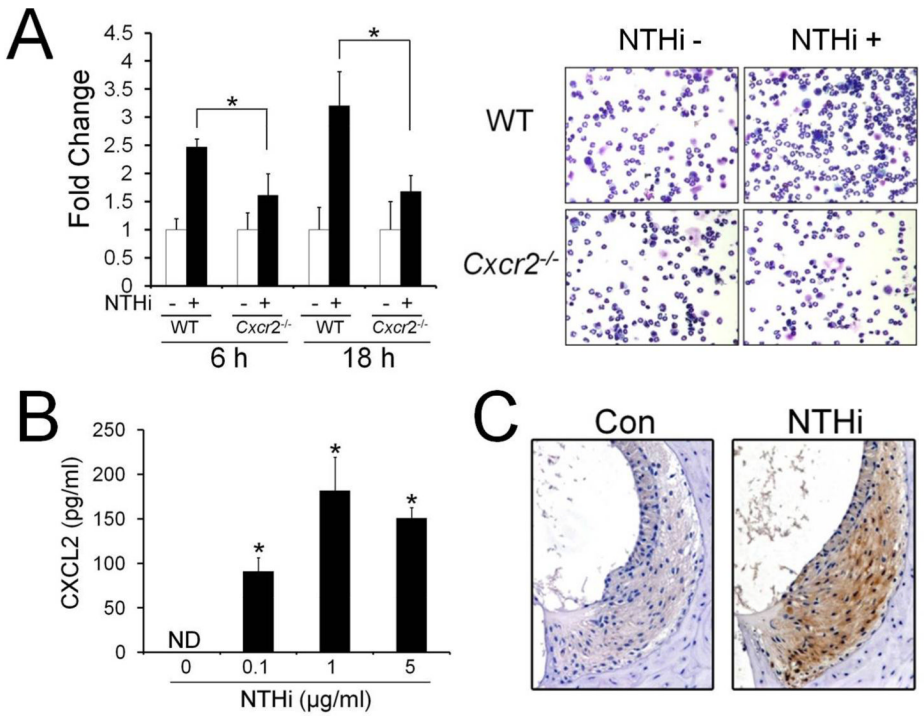

FIGURE 1.

SLFs up-regulate CXCL2 in response to NTHi. *A*, Migration assays show that CXCR2 deficiency inhibits migration of PMNs in response to the NTHi-induced SLF-derived molecules. WT: wild-type PMNs, *Cxcr2*$^{-/-}$: CXCR2-deficient PMNs, NTHi-: conditioned medium from the NTHi-unexposed RSL cells, NTHi+: conditioned medium from the NTHi-exposed RSL cells. *B*, ELISA analysis shows that the RSL cells up-regulate CXCL2 in response to NTHi. ND: not detected. The experiments were performed in triplicate and repeated twice. Values are given as the mean ± standard deviation ($n = 3$). *: $p < 0.05$. *C*, Immunolabeling shows that CXCL2 is highly expressed in the spiral ligament of the NTHi-inoculated mice (NTHi), but not in the saline-inoculated mice (Con). Original magnification: x50.

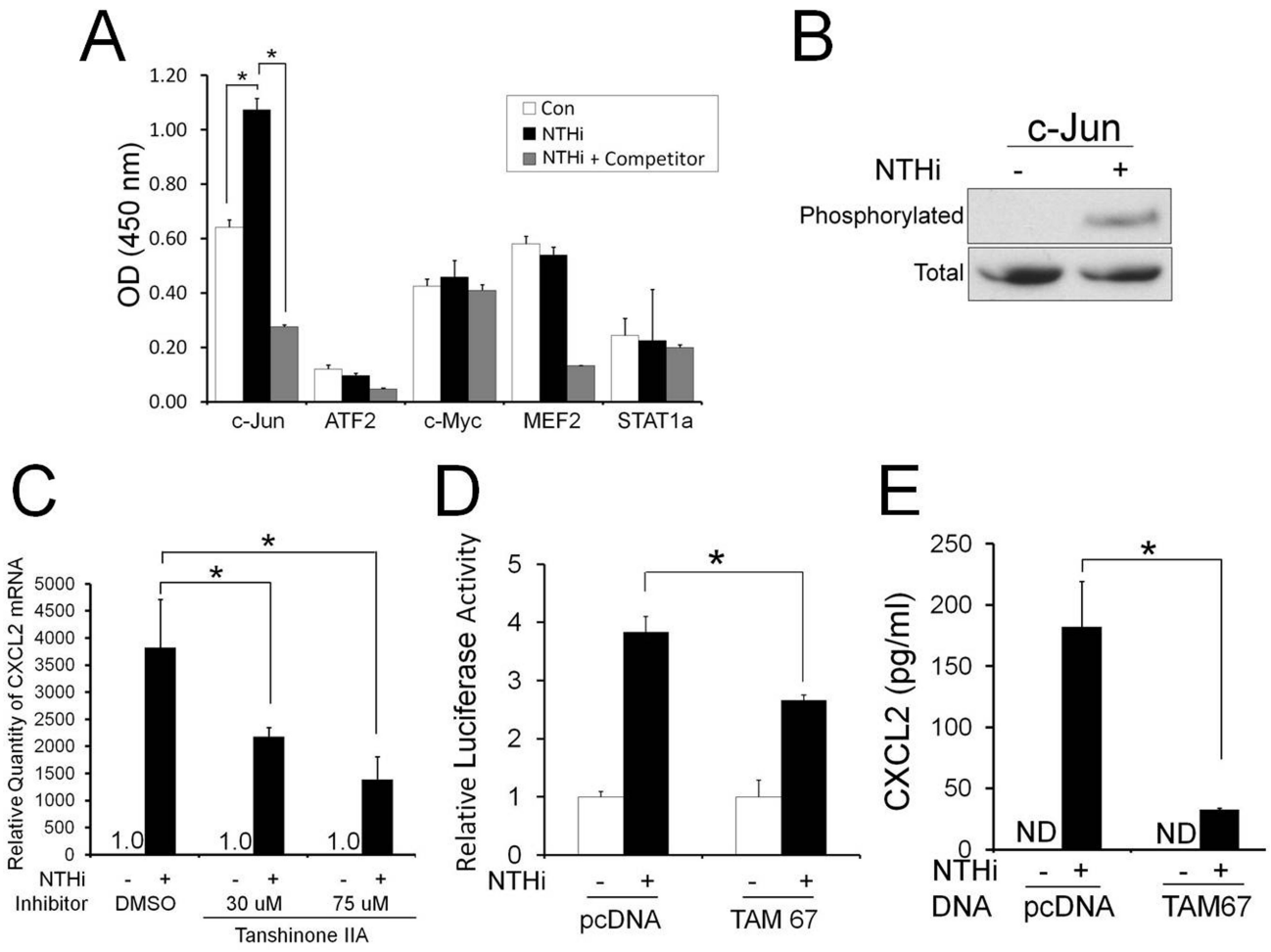

FIGURE 2.

Activation of the c-Jun is required for NTHi-induced CXCL2 up-regulation. *A*, Transcription factor ELISAs show that the SLFs activate c-Jun in response to NTHi. *B*, Phosphorylation assays show that c-Jun of the nuclear fraction is phosphorylated in response to NTHi. *C*, NTHi-induced CXCL2 up-regulation is noted to be inhibited by Tanshinone IIA in a dose-dependent manner. *D*, Luciferase assays demonstrate that a dominant-negative inhibition of c-Jun (TAM 67) suppresses NTHi-induced CXCL2 up-regulation. *E*, ELISA analysis shows that a dominant-negative inhibition of c-Jun (TAM 67) markedly suppresses NTHi-induced CXCL2 up-regulation. ND: not detected. pcDNA: a mock transfection. Results were expressed as fold-induction, taking the value of the non-treated group as 1. The experiments were performed in triplicate and repeated twice. Values are given as the mean ± standard deviation ($n = 3$). *: $p < 0.05$.

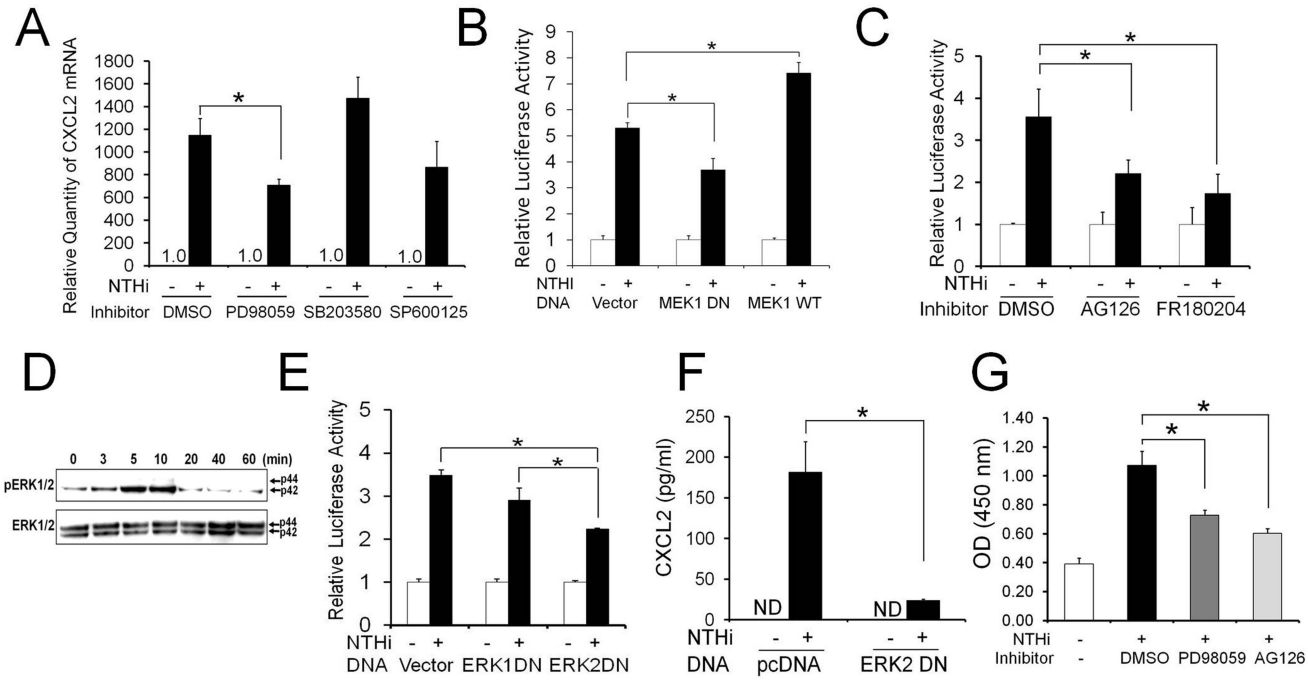

FIGURE 3.

MEK1-ERK2 signaling is required for NTHi-induced activation of c-Jun resulting in CXCL2 up-regulation in SLFs. *A*, Quantitative RT-PCR analysis shows that NTHi-induced CXCL2 up-regulation is inhibited by PD98059, a MEK inhibitor, not by other MAPK inhibitors. *B*, Luciferase assays demonstrate that a dominant-negative inhibition of MEK1 suppresses NTHi-induced CXCL2 up-regulation, but is enhanced by the over-expression of the wild type of MEK1. Vector: a mock transfection. *C*, NTHi-induced CXCL2 up-regulation is noted to be inhibited by AG126 and FR180204. *D*, Phosphoylation assays shows that the SLFs activates ERK in response to NTHi, peaked around 10 min after exposure. Note that ERK2 (p42), not ERK1 (p44), is mainly phosphorylated upon exposure to NTHi in the SLFs. *E*, Luciferase assays show that NTHi-induced CXCL2 up-regulation is suppressed by a dominant-negative inhibition of ERK2, but not by ERK1. *F*, ELISA analysis shows that a dominant-negative inhibition of ERK2 significantly suppresses NTHi-induced CXCL2 up-regulation. ND: not detected. pcDNA: a mock transfection. *G*, Transcription factor ELISAs show that NTHi-induced activation of c-Jun is inhibited by PD98059 and AG126. OD: optical density. Results were expressed as fold-induction, taking the value of the non-treated group as 1. The experiments were performed in triplicate and repeated twice. Values are given as the mean ± standard deviation ($n = 3$). *: $p < 0.05$.

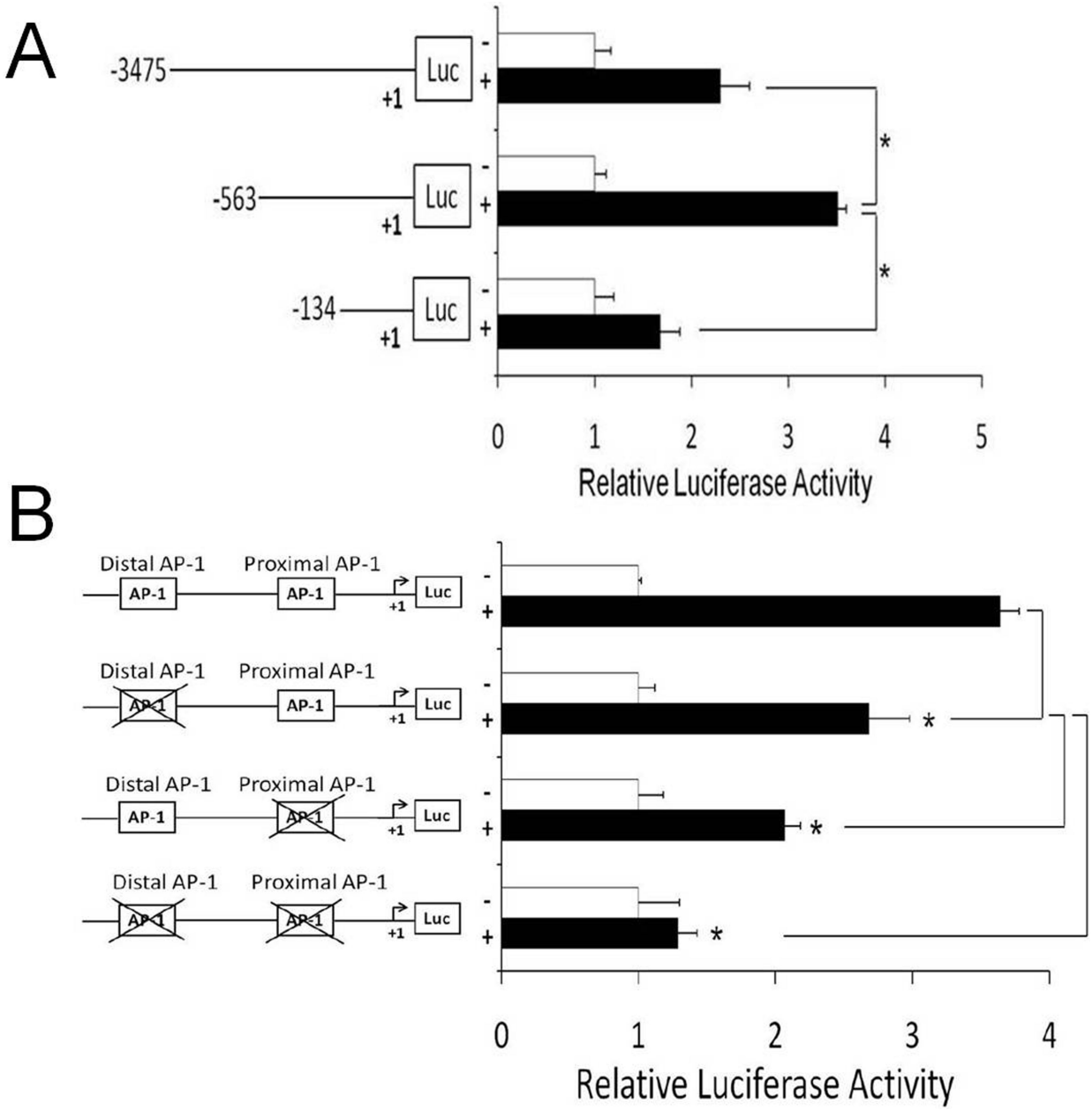

FIGURE 4.

The AP-1 motif is critically involved in NTHi-induced CXCL2 up-regulation. *A*, Luciferase assays using nested deletions show that the NTHi-responsive element is located between -564 and -134 of the rat CXCL2 promoter region. *B*, Luciferase assays with site-directed mutagenesis show that the mutation of the proximal AP-1 motif inhibits NTHi-induced CXCL2 up-regulation more than that of the distal AP-1 motif. Mutation of both AP-1 motifs is noted to completely inhibit NTHi-induced CXCL2 up-regulation. Results were expressed as fold-induction, taking the value of the non-treated group as 1. The experiments were performed in triplicate and repeated twice. Values are given as the mean ± standard deviation ($n = 3$). *: $p < 0.05$.

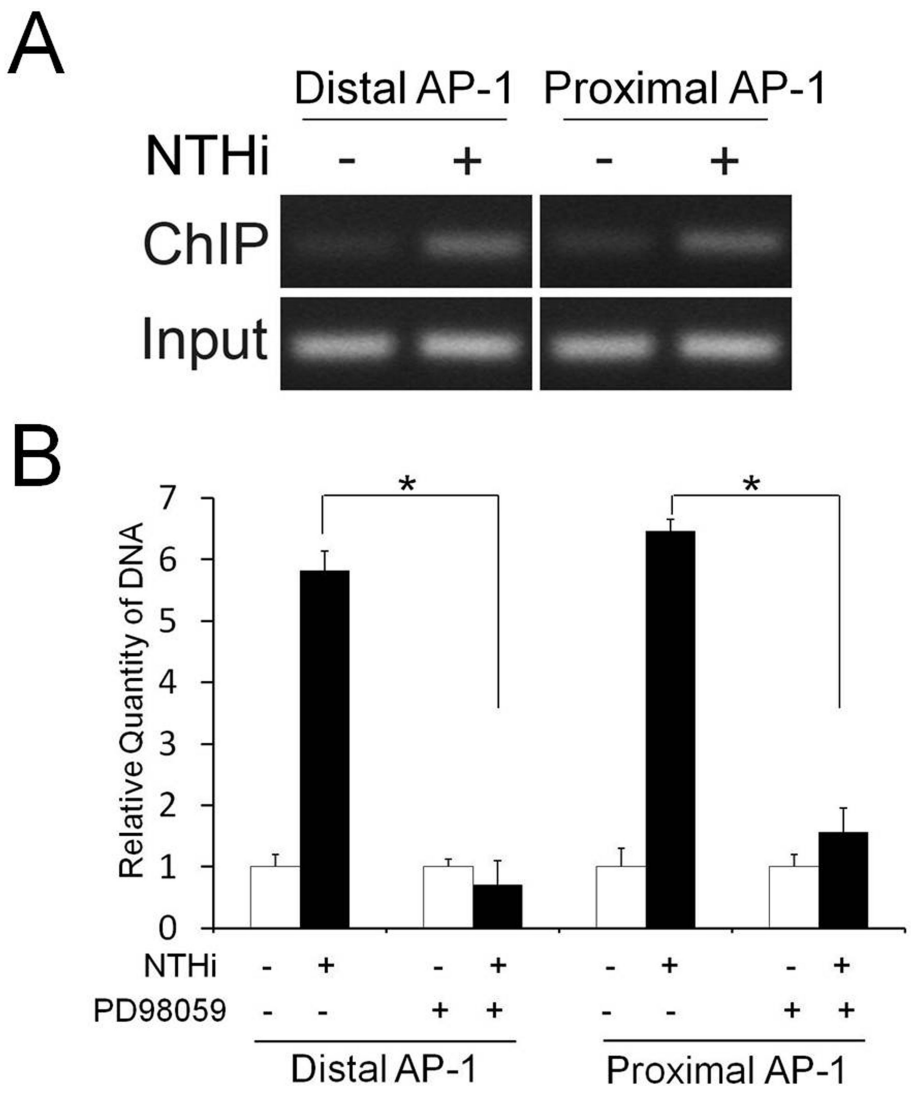

FIGURE 5.

NTHi-activated c-Jun binds the AP-1 motifs of CXCL2. *A*, ChIP-PCR analysis shows that c-Jun binds the AP-1 motifs of CXCL2 in response to NTHi. *B*, ChIP-qPCR analysis shows that PD98059 inhibits NTHi-induced binding of c-Jun to both AP-1 motifs. Results were expressed as fold-induction, taking the value of the non-treated group as 1. The experiments were performed in triplicate and repeated twice. Values are given as the mean ± standard deviation ($n = 3$). *: $p < 0.05$.

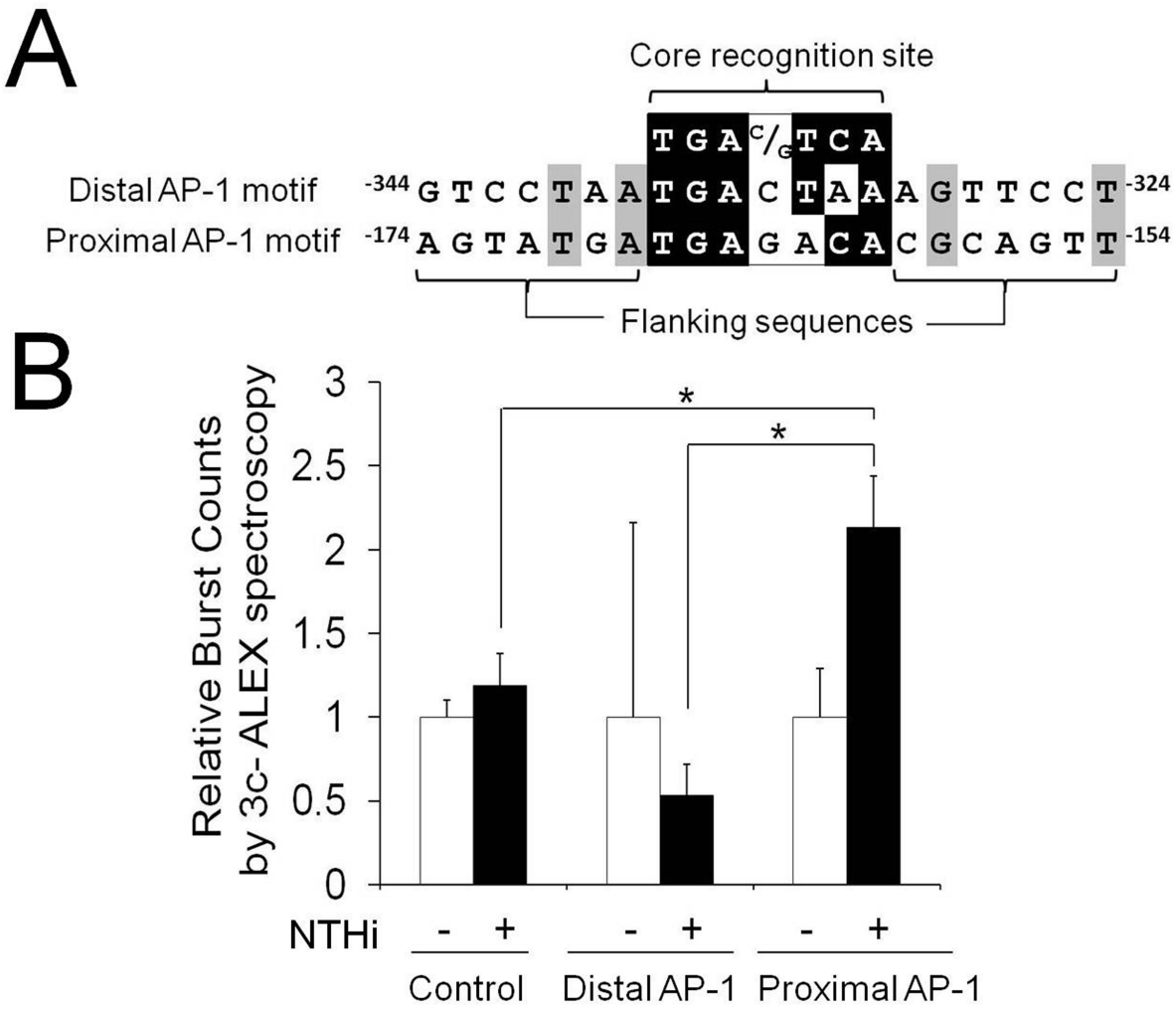

FIGURE 6.

The proximal AP-1 motif has a higher binding affinity to c-Jun/DNA binding than the distal one in vitro. *A*, Sequence alignment analysis showing a difference between the distal and proximal AP-1 motifs. *B*, ALEX fluorescence spectroscopy shows that the proximal AP-1 motif has a higher binding affinity to NTHi-activated c-Jun than the distal one in vitro. Results were expressed as fold-induction, taking the value of the non-treated group as 1. The experiments were performed in triplicate and repeated twice. Values are given as the mean ± standard deviation ($n = 3$). *: $p < 0.05$.